JOURNAL OF NATURAL PRODUCTS

Note

pubs.acs.org/jnp

Unrestrained Conformational Characterization of *Stenocereus eruca* Saponins in Aqueous and Nonaqueous Solvents

Conrado Pedebos, Laercio Pol-Fachin, and Hugo Verli*

Centro de Biotecnologia, Universidade Federal do Rio Grande do Sul, Avenida Bento Gonçalves 9500, CP 15005, Porto Alegre, 91500-970, RS, Brazil

Supporting Information

ABSTRACT: Saponins are secondary metabolites that have a plethora of biological activities. However, the absence of knowledge of their 3D structures is a major drawback for structural-based strategies in medicinal chemistry. To address this problem, the current work presents structural models of *Stenocereus eruca* saponins, named erucasaponin A and stellatoside B. These compounds were constructed on the basis of a combination of unrestrained molecular dynamics (MD) simulations and NOESY data, in both pyridine and water. The models obtained in this way offer a robust description of the saponin dynamics in solution and support the use of submicrosecond MD simulations in describing and predicting glycoconjugate conformations.

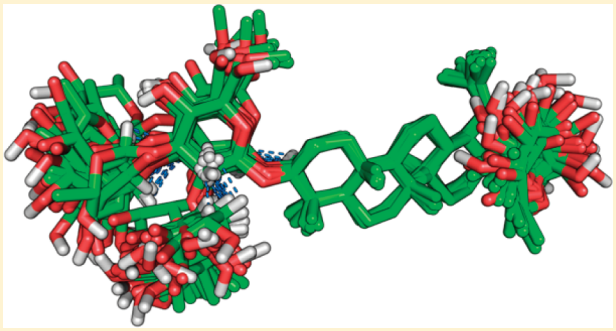

Saponins are glycosides that are usually derived from plants and are composed of a hydrophobic aglycone moiety (triterpene or steroid) and one or several hydrophilic saccharide chains. Such compounds have been shown to present many properties of potential pharmacological use, such as antitumoral, antiviral, anti-inflammatory, antinociceptive, and antithrombotic activities.[1] Erucasaponin A (**1**) and stellatoside B (**2**) are two saponins that are extracted from *Stenocereus eruca*, a member of the Cactaceae family. It is endemic to the Sonoran desert, which is located in the province of Baja California Sur, Mexico.[2] Although these biomolecules have not been shown to have any of the above-mentioned activities, the erucasaponin A pentacyclic lupane-type triterpene, betulinic acid, has been shown to possess anti-HIV-1 activity[3] and cytotoxicity against certain tumor cell lines.[4] Moreover, this triterpene displays antimalarial,[5] antimicrobial,[6] and anti-inflammatory activities,[7] among others.[3]

Such activities usually depend on a ligand−receptor recognition process, a dynamical phenomenon dependent on the flexibility of both molecules.[8] Therefore, the characterization of their solution conformational ensemble is a necessary step toward a deeper understanding of the determinants, at the atomic level, for compounds' biological activity and, consequently, for a more efficient design of new bioactive compounds.[9] Accordingly, a structural characterization of saponins through NMR methods could provide information about their conformational ensemble if a reasonable amount of NOE contacts are obtained.[10] However, because of the high flexibility of their linked carbohydrate chains[10−12] and the multiple conformers coexisting in solution for such molecules,[10,12−16] it is usually challenging to obtain 3D models for glycoconjugates. Additionally, the environment in which the NMR experiments are performed does not necessarily correspond to that of physiological solutions. In a previous study, both *S. eruca* saponins,[17] **1** and **2**, had their structure elucidated in pyridine, a heterocyclic and aromatic solvent.

Considering the lack of consistent and fast approaches for obtaining 3D models of saponins and other glycoconjugates that properly describe the solution and biological conformational states, the present work aims to analyze and characterize, at the atomic level, compounds **1** and **2** with respect to their structure and dynamics in a nonaqueous solvent (pyridine) through unrestrained MD simulations, which were further validated through inter-residue NOE contacts. Based on the adequacy of the obtained structures, original models for these saponins were proposed in H_2O, thus providing insights on the saponins' conformational pattern in a biologically similar environment.

Because saponin structures are usually assessed by NMR methods in nonaqueous solutions, a pyridine box was constructed and simulated to mimic an environment in which erucasaponin A (**1**) and stellatoside B (**2**) were studied.[17] Only a small number of studies have previously simulated similar pyridine systems,[18−21] but force fields other than GROMOS96, such as OPLS/AA, AMBER, and CHARMM, have been used. Therefore, an MD simulation of 0.1 μs was performed in 310 K to stabilize the box. The physical chemistry parameters chosen in the comparison were the enthalpy of vaporization (ΔH_{vap}) and the density (d) of the system. The ΔH_{vap} was calculated using the following equation:

Received: January 13, 2012
Published: June 13, 2012

dx.doi.org/10.1021/np3000393 | *J. Nat. Prod.* 2012, 75, 1196−1200

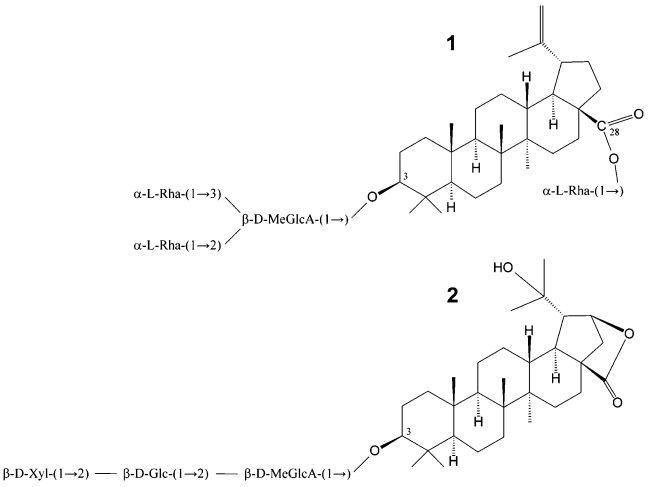

$$\Delta H_{vap} = E_{pot(g)} - E_{pot(l)} + RT$$

where $E_{pot(g)}$ is the potential energy of a single pyridine molecule in a vacuum and $E_{pot(l)}$ is the (potential energy$_{box}$)/(number of molecules). The result obtained for the density of the system was 0.9835 ± 0.0070 g/mL, the calculated enthalpy of vaporization was 33.3 ± 4.0 kJ/mol, and the heat capacity was 140.0 ± 3.7 J/mol·K. This result indicates that the density values were in good agreement with experimental data (0.9819 g/mL),[22] while the enthalpy of vaporization was slightly underestimated (40.2 kJ/mol) and the heat capacity a bit overestimated (134.9 J/mol·K).[23]

On the basis of the structures of compounds **1** and **2**, seven glycosidic linkages were studied: β-D-Xyl-(1→2)-Glc, β-D-Glc-(1→2)-MeGlcA, β-D-MeGlcA-(1→3)-Stln, α-L-Rha-(1→2)-MeGlcA, α-L-Rha-(1→3)-MeGlcA, β-D-MeGlcA-(1→3)-BetA, and α-L-Rha-(1→28)-BetA. The energy contour plots generated for such linkages (Figure 1) indicate that multiple minimum energy conformations might coexist, especially in the saccharidic moieties because of their high flexibility. The data obtained in the contour plots also demonstrate that the conformational ensemble adopted by the molecule is more strongly influenced by its glycosidic linkage pattern, such as (1→2) or (1→3), than by the residues involved in the linkage. While small variations could occur, the main minimum-energy regions still remain within similar conformations. Furthermore, the presence of an explicit solvent (pyridine) showed a discrete effect in comparison with its vacuum conformational profile, mostly populating geometries around the vacuum minimum energy regions with only minor exceptions. Similar conformational behaviors could be observed for those disaccharides in other nonaqueous solvents (MeOH and EtOH), as well as in H_2O (Supporting Information, Tables S1 and S2), which suggests that the studied solvents are mostly not capable of promoting the population of new conformational states, not observed from vacuum energy maps.

The most abundant conformational states of each glycosidic linkage were then employed as starting geometries for the construction of complete models of compounds **1** and **2**, which was previously demonstrated to be a successful approach to obtain solution-like, NMR-validated, glycan chains.[12,16,24,25] Subsequent to MD simulations of the complete saponins, a comparison between the conformational profile adopted by the isolated (disaccharidic or monosaccharide-aglycone) glycosidic linkages and their behavior when composing the complete saponins was performed in pyridine (Table 1) and under other nonaqueous solvents (MeOH and EtOH, Supporting Information, Tables S1 and S2).[26−31] As a general feature, no major differences could be observed between the two evaluated complexity levels, indicating that the saponin glycosidic linkages do not adopt new conformational states in relation to their isolated forms, but present different relative abundances. Furthermore, the glycosidic linkage shared by both saponins, β-D-MeGlcA-(1→3)-triterpene, showed the same conformational profile when isolated in solution, independent of the aglycone, suggesting that the size of the aglycone has minor conformational influence on the studied compounds. However, the attachment of rhamnose residues, particularly the 1→3-linked, to the glucuronic acid in compound **1** is capable of modifying the conformational profile of their vicinal glycosidic linkages. Moreover, while all glycosidic linkages evaluated showed agreement with the exoanomeric effect (supplementary note 1),[32,33] the conformational profiles obtained from our MD simulations are comparable to the $\phi-\psi$ glycosidic linkage geometries obtained by previous reports on similar disaccharide

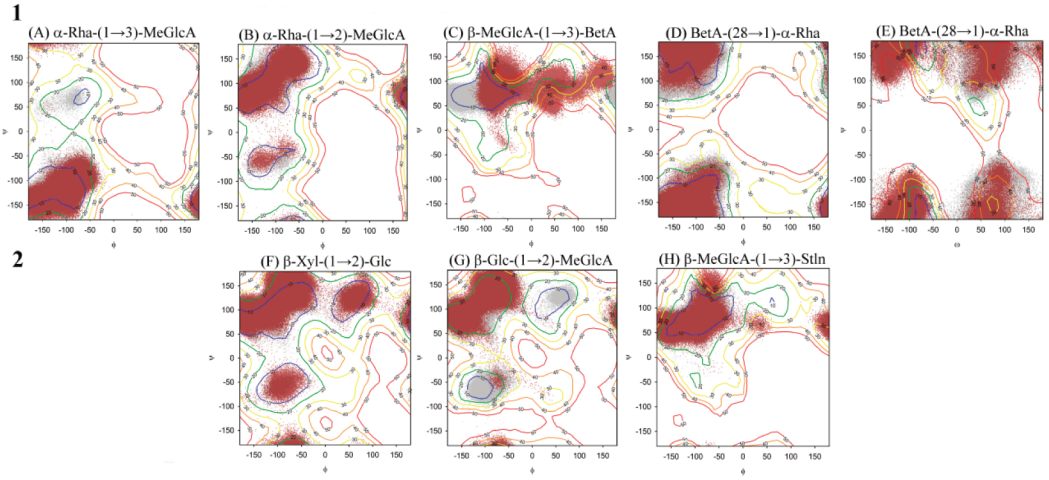

Figure 1. Contour plots of the disaccharide units from compounds **1** (A−E) and **2** (F−H). The vacuum energy maps are shown for every 10 kJ/mol, from −10 to 50 kJ/mol, and superimposed are the geometries of the population in pyridine as isolated disaccharides (gray dots) and as the complete saponin (dark red dots), extracted from 0.1 μs MD simulations.

dx.doi.org/10.1021/np3000393 | J. Nat. Prod. 2012, 75, 1196−1200

Table 1. Comparison of the Dihedral Angles of the Glycosidic Linkages from Compounds 1 and 2 in Their Isolated (Disaccharidic or Monosaccharide-Aglycone) Units and the Complete Saponins Obtained from MD Simulation Data in Pyridine

		dihedral angle (deg)					
		isolated			complete		
compound	glycosidic linkage	ϕ	ψ	ω	ϕ	ψ	ω
1	α-L-Rha-(1→3)-β-D-MeGlcA	−107 ± 36	−109 ± 30		−111 ± 37	−120 ± 25	
	α-L-Rha-(1→2)-β-D-MeGlcA	−111 ± 42	108 ± 40		−142 ± 39	92 ± 30	
	β-D-MeGlcA-(1→3)-BetA	−108 ± 36	85 ± 21		−52 ± 39	88 ± 16	
	α-L-Rha-(1→28)-BetA	−131 ± 49	−159 ± 31	53 ± 55	−105 ± 38	−157 ± 29	−79 ± 70
2	β-D-Xyl-(1→2)-β-D-Glc	−81 ± 53	119 ± 32		−80 ± 64	120 ± 41	
	β-D-Glc-(1→2)-β-D-MeGlcA	−98 ± 42	91 ± 66		−102 ± 30	127 ± 28	
	β-D-MeGlcA-(1→3)-Stln	−108 ± 34	85 ± 22		−120 ± 37	69 ± 17	

units (Supporting Information, Table S1),[26−31] reinforcing the capability of the employed protocol to predict glycoconjugate conformations in solution.

Both compounds **1** and **2** have been previously characterized by NMR spectroscopy. Their interproton NOE contacts derived from such methods were used in the validation of the obtained conformational ensemble from the MD simulations (Table 2). For **1**, the contacts observed are between H-1 (from the 1→3 linked α-L-Rha) and H-3 (from the β-D-MeGlcA), H-1 (from the 1→2 α-L-Rha) and H-2 (from the β-D-MeGlcA), and H-1 (from the β-D-MeGlcA) and H-3 (from BetA). With respect to **2**, although no NOE contacts have been reported between different monosaccharide residues and between them and the aglycone, we observed potential contacts between H-1 (from the β-D-Xyl) and H-2 (from the β-D-Glc), H-1 (from the β-D-Glc) and H-2 (from the β-D-MeGlcA), and H-1 (from the β-D-MeGlcA) and H-3 (Stln). In fact, employing different solvents, trans glycosidic contacts have been observed recently in data reported elsewhere[34] for similar or identical glycan moieties, between β-D-Glc H-1 and β-D-MeGlcA H-2, as well as between β-D-MeGlcA H-1 and Stln H-3 (Supporting Information, Table S3).

Table 2. Comparison between NOE Contacts of Compound 1 and the Interproton Distances Derived from MD Simulations

saponin	proton of residue 1	proton of residue 2	interproton distance from MD (Å)
1	1→3 linked α-L-Rha H-1	β-D-MeGlcA H-3	2.24 ± 0.37
	1→2 linked α-L-Rha H-1	β-D-MeGlcA H-2	2.44 ± 0.41
	β-D-MeGlcA H-1	BetA H-3	2.61 ± 0.46

The conformational profile of the carbohydrate residues is connected to the behavior of the glycosidic linkages.[35] Thus, to properly evaluate the conformations that are adopted by both compounds, a description of the most populated geometries of each glycosidic linkage was performed (Figure 2) in the two simulated solutions (pyridine and H_2O). Accordingly, when compared to the pyridine solution, the aqueous medium does not promote new conformational states. On the other hand, compound **2** presented a higher flexibility than **1**, as indicated by variations on their conformational profile along with larger

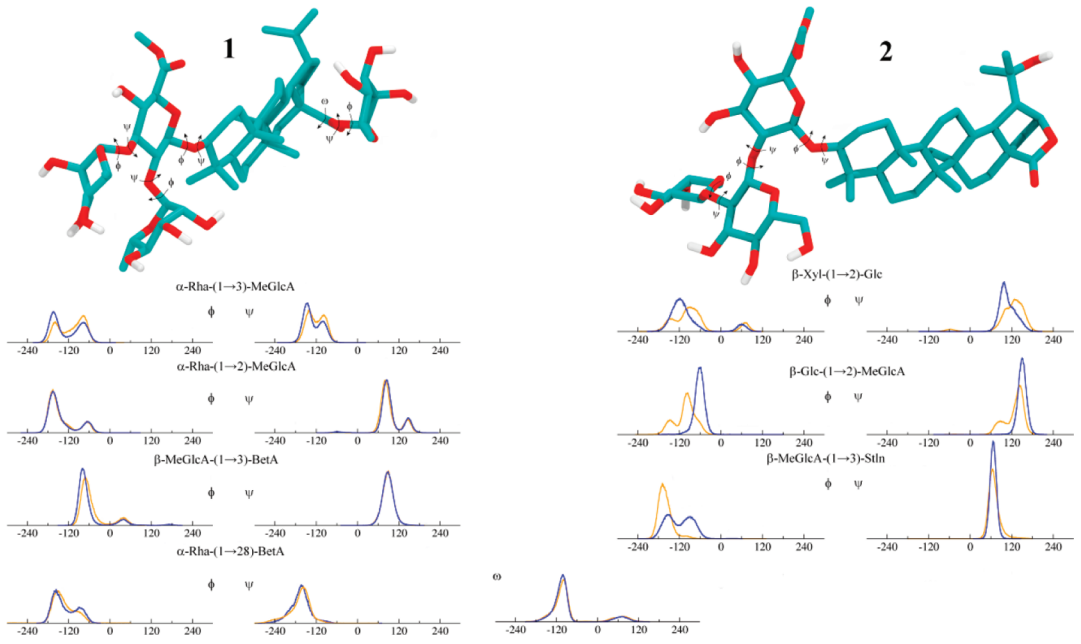

Figure 2. Distribution of the ϕ, ψ, and ω dihedral angles that are associated with the glycosidic linkages composing compounds **1** and **2**. The nonaqueous solution (pyridine) is indicated in orange, and the aqueous solution is represented in blue.

dx.doi.org/10.1021/np3000393 | J. Nat. Prod. 2012, 75, 1196−1200

standard deviations in the average glycosidic linkage geometries. A root mean square fluctuation (RMSf) analysis in pyridine generated a 0.177 ± 0.076 nm variation for **1**, while there was a 0.203 ± 0.108 nm variation for **2**. Additionally, the pyridine solvent was also capable of allowing a higher flexibility for **2** because the geometry distribution in this solvent demonstrated the existence of additional conformational states, which were absent in water, as perceived in the ϕ and ψ distributions of β-D-Xyl-(1→2)-β-D-Glc and β-D-Glc-(1→2)-β-D-MeGlcA and in the ϕ distribution of β-D-MeGlcA-(1→3)-Stln. A RMSf analysis in aqueous solution demonstrated a slightly higher flexibility for **1**, as indicated by the 0.230 ± 0.092 nm variation that was obtained, while for **2**, this environment significantly reduced its flexibility, as indicated by the 0.131 ± 0.060 nm variation that was detected. These data could indicate a reason for the nonidentification of any inter-residue NOE contacts in nonaqueous solution for **2** and the identification of these possible contacts for **1** .

An understanding of solvation in compound dynamics and conformations is crucial for achieving a precise picture of ligand interactions with their respective target receptors,[10] which most likely rises in importance as the flexibility of the compounds increases. In flexible glycoconjugates such as saponins, such a characterization is not a simple process and demands the use of high-field NMR spectroscopy.[36,37] Still, the saccharidic portion remains a challenge because its high flexibility usually impairs the crystallization process and could induce the presence of virtual conformations in NMR.[10] Additionally, the nonobservance of NOE signals or the presence of few signals creates great difficulties in obtaining a solution characterization of these molecules' conformation.[10] Therefore, MD simulations emerge as promising, fast, and low-cost tools aiming to describe and predict the conformational ensembles adopted by carbohydrates.[12,16,23,24,38,39]

In the present work, two saponins had their structure constructed from their constituent glycosidic linkages' most abundant conformational states. These initial models were subjected to refinement under unrestrained MD simulations in both pyridine and H_2O and were further compared to experimental data. Upon reproducing NOESY signals observed in pyridine solvent, the data obtained suggest that submicrosecond-long MD simulations could represent important tools for generating biologically relevant atomic models for flexible biomolecules such as saponins.

EXPERIMENTAL SECTION

Nomenclature, Topologies, and Software. The IUPAC recommendations and symbols of nomenclature[40] were adopted. The orientation of two contiguous carbohydrate residues, or a monosaccharide and a triterpene, was properly described with their glycosidic linkage torsional angles. For a (1→X) linkage, where "X" is "2", "3", or "28" for the (1→2), (1→3), or (1→28), respectively, the ϕ and ψ dihedral angles are defined as shown in eqs 1 and 2:

$$\phi = \text{O-5} - \text{C-1} - \text{O-1} - \text{C-X} \quad (1)$$

$$\psi = \text{C-1} - \text{O-1} - \text{C-X} - \text{C-(X-1)} \quad (2)$$

For a (1→28) linkage, omega (ω) is defined as below:

$$\omega = \text{O-28A} - \text{C-28} - \text{C-17} - \text{C-16} \quad (3)$$

The topologies for saccharides and triterpene have been generated by the PRODRG server.[41] Structures were manipulated using PyMOL[42] and MOLDEN.[43] All of the MD simulations and analyses were performed using the GROMACS simulation suite, version 3.3.3,[44] and the GROMOS96 43a1 force field.[45]

Building Blocks and Topology Construction. To obtain reasonable starting geometries for the saponins' conformational studies, the building block methodology[46] was applied. Specifically, each compound was constructed on the basis of the most prevalent conformations of its minimal components in solution (disaccharides or linkages between a monosaccharide and a triterpene). Accordingly, all of the units were constructed using the MOLDEN software and were submitted to the PRODRG server to retrieve their crude topologies and atomic coordinates. Additional refinements were added to such topologies, including HF/6-31**-derived Löwdin atomic charges, as obtained from previous studies,[38] or calculated, in the case of the methyl ester (C-6 = 0.290, O-6A = −0.225, O-6B = −0.300, and C-7 = 0.235) and the (1→28) linkage (C-17 = −0.084, C-28 = 0.393, O-28A = −0.303, O-28B = −0.292, and C-1 = 0.286) atomic charges. Improper dihedrals were added to maintain the conformational states $^1C_4$ for all α-L-rhamnose (α-L-Rha) and $^4C_1$ for β-D-xylose (β-D-Xyl), β-D-glucose (β-D-Glc), and methyl β-D-glucuronate (β-D-MeGlcA) residues. Additionally, proper dihedrals were included, as described in the GROMOS96 force field. Moreover, the pyridine topology was constructed on the basis of the parameters and charges presented in the GROMOS96 43a1 force field for phenylalanine, while the nitrogen charge used was taken from the imidazole of the histidine side-chain.

Contour Plots. A conformational description for each disaccharidic or monosaccharide-aglycone linkage in compounds **1** and **2** was obtained by rotating their glycosidic linkage torsion angles between −180° and 150°, in steps of 30°, thus generating 144 conformers for each pair of torsions. These calculations were performed using a constant force to restrict the ϕ and ψ proper dihedrals in the energy minimization process, allowing the exploration of the conformational space associated with the block's given linkages.[25] The minimized conformations were further submitted to a series of MD simulations for 20 ps at 10 K, with an integration step of 0.5 fs, thus improving the search for minimum-energy conformations. The relative stability of each conformer was then used for constructing the relaxed contour plots that describe each glycosidic linkage conformation.

MD Simulations. The geometries identified as the minimum-energy conformations, which were obtained from the energy contour plots, as well as the complete saponin models, were employed as starting conformations for unrestrained MD simulations for 0.1 μs in pyridine or aqueous solutions (SPC water model)[47] and in a solvated cubic box using periodic boundary conditions. Counterions (Na^+) were used to neutralize the system, if necessary. To constrain covalent bond lengths, the LINCS method[48] was applied, therefore allowing an integration step of 1 fs after a first energy minimization by using the steepest descent algorithm. The particle mesh Ewald method[49] was used in the calculation of electrostatic interactions. Temperature and pressure were kept constant by coupling carbohydrates, triterpenes, saponins, ions, and solvent to external temperature and pressure baths with coupling constants of τ = 0.1 and 0.5 ps,[50] respectively. The dielectric constant used was ε = 1.

NOESY Signals. The calculations performed in this work are based on a united-atom force field, which significantly reduces computational costs,[51] thus allowing faster simulations with longer time scales. Therefore, to allow a comparison of the simulations to previous experimental data (that is, NOE contacts),[17] nonpolar hydrogen atoms were added to frames retrieved from the nonaqueous trajectories, at every 10 ps, for each saponin. The apolar hydrogens presented in the analysis were H-1 (linked to C-1), H-2 (linked to C-2), and H-3 (linked to C-3) of the monosaccharides and the triterpene. The expected hybridization and geometries for these atoms were respected, and the final models, containing hydrogen atoms, were used to calculate the average interatomic distances used for comparison to the available NOESY signals data.

ASSOCIATED CONTENT

Supporting Information

Figures and tables for dihedral distribution of glycosidic linkages from compounds **1** and **2** in EtOH and MeOH, and a table concerning the trans glycosidic H−H contacts involving

dx.doi.org/10.1021/np3000393 | J. Nat. Prod. 2012, 75, 1196−1200

compound **2**. This material is available free of charge via the Internet at http://pubs.acs.org.

AUTHOR INFORMATION

Corresponding Author

*Tel: +55-51-33087770. Fax: +55-51-33087309. E-mail: hverli@cbiot.ufrgs.br.

Notes

The authors declare no competing financial interest.

ACKNOWLEDGMENTS

This work was supported by Conselho Nacional de Desenvolvimento Científico e Tecnológico (CNPq), MCT, by Coordenação de Aperfeiçoamento de Pessoal de Nível Superior (CAPES), MEC, Brasília, DF, Brazil, and the Fundação de Amparo à Pesquisa do Estado do Rio Grande do Sul (FAPERGS).

REFERENCES

(1) Mauricio, I.; Francischetti, B.; Monteiro, R. Q.; Guimarães, J. A. *Biochem. Biophys. Res. Commun.* **1997**, *235*, 259−263.
(2) Clark-Tapia, R.; Mandujano, M. C.; Valverde, T.; Mendoza, A.; Molina-Freaner, F. *Biol. Control* **2005**, *124*, 123−132.
(3) Fujioka, T.; Kashiwada, Y.; Kilkusie, R. E.; Cosentino, L. M.; Ballas, L. M.; Jiang, J. B.; Janzen, W. P.; Chen, I. S.; Lee, K. H. *J. Nat. Prod.* **1994**, *57*, 243−247.
(4) Cichewicz, R. H.; Kouzi, S. A. *Med. Res. Rev.* **2004**, *24*, 90−114.
(5) Steele, J. C. P.; Warhurst, D. C.; Kirby, G. C.; Simmonds, M. S. J. *Phytother. Res.* **1999**, *13*, 115−119.
(6) Nick, A.; Wright, A. D.; Rali, T.; Sticher, O. *Phytochemistry* **1995**, *40*, 1691−1695.
(7) Safayhi, H.; Sailer, E.-R. *Planta Med.* **1997**, *63*, 487−493.
(8) Spiwok, V.; Hlat-Glembová, K.; Tvaroska, I.; Králová, B. *J. Chem. Inf. Model.* **2012**, *52*, 804−813.
(9) Schneider, G. *Nat. Rev. Drug Discovery* **2010**, *9*, 273−276.
(10) Woods, R. J. *Glycoconjugate J.* **1998**, *15*, 209−216.
(11) Dwek, R. A. *Chem. Rev.* **1996**, *96*, 683−720.
(12) Fernandes, C. L.; Sachett, L. G.; Pol-Fachin, L.; Verli, H. *Carbohydr. Res.* **2010**, *345*, 663−671.
(13) Cumming, D. A.; Carver, J. P. *Biochemistry* **1987**, *26*, 6664−6676.
(14) Wormald, M.; Petrescu, A.-J.; Pao, Y.-L.; Glythero, A.; Elliot, T.; Dwek, R. A. *Chem. Rev.* **2002**, *102*, 371−387.
(15) Pérez, S.; Mulloy, B. *Curr. Opin. Struct. Biol.* **2005**, *15*, 517−524.
(16) Pol-Fachin, L.; Fernandes, C. L.; Verli, H. *Carbohydr. Res.* **2009**, *344*, 491−500.
(17) Okazaki, S.; Kinoshita, K.; Koyama, K.; Takahashi, K.; Yuasa, H. *J. Nat. Med.* **2007**, *61*, 24−29.
(18) Ghatee, M. H.; Zolghadr, A. R.; Moosavi, F.; Pakdel, L. *J. Chem. Phys.* **2011**, *134*, 1−14.
(19) Baker, C. M.; Grant, G. H. *J. Chem. Theory Comput.* **2007**, *3*, 530−548.
(20) Jorgensen, W. L.; McDonald, N. A. *J. Mol. Struct. (THEOCHEM)* **1998**, *424*, 145−155.
(21) Caleman, C.; van Mareen, P. J.; Hong, M.; Hub, J. S.; Costa, L. T.; van der Spoel, D. *J. Chem. Theory Comput.* **2012**, *8*, 61−74.
(22) Lide, D. R. *Handbook of Chemistry and Physics*; 2003; C-462 and C-672.
(23) Parks, G. S.; Todd, S. S.; Moore, W. A. *J. Am. Chem. Soc.* **1936**, *58*, 398−401.
(24) Pol-Fachin, L.; Serrato, R. V.; Verli, H. *Carbohydr. Res.* **2010**, *345*, 1922−1931.
(25) Pol-Fachin, L.; Verli, H. *Carbohydr. Res.* **2008**, *343*, 1435−1445.
(26) Woods Group. (2005−2012) GLYCAM Web. Complex Carbohydrate Research Center, University of Georgia, Athens, GA (http://www.glycam.com).
(27) Frank, M.; Lütteke, T.; Von der Lieth, C.-W. *Nucleic Acids Res.* **2007**, *35*, D287−D290.
(28) Somers, W. S.; Tang, J.; Shaw, G. D.; Camphausen, R. T. *Cell* **2000**, *103*, 467−479.
(29) Jansson, P.-E.; Widmalm, G. *J. Chem. Soc., Perkin Trans. 2* **1992**, *7*, 1085−1090.
(30) Ohanessian, J.; Longchambom, F.; Arene, F. *Acta Crystallogr.* **1978**, *B34*, 3666−3671.
(31) Rivet, A.; Sabin, Ch.; Mazeau, K.; Imberty, A.; Pérez, S. A. Database of 3-Dimensional Structures of Disaccharides 2001, http://www.cermav.cnrs.fr/cgi-bin/di/di.cgi.
(32) Rao, V. S. R.; Qasba, P. K.; Balaji, P. V.; Chandrasekaran, R. In *Conformation of Carbohydrates*; Rao, V. S. R., Ed.; Harwood Academic: The Netherlands, 1998; pp 91−130.
(33) Woods, R. J.; Dwek, R. A.; Edge, C. J.; Fraser-Reid, B. *J. Phys. Chem.* **1995**, *99*, 3832−3846.
(34) Okazaki, S.; Kinoshita, K.; Ito, S.; Koyama, K.; Yuasa, H.; Takahashi, K. *Phytochemistry* **2011**, *72*, 136−146.
(35) Imberty, A.; Perez, S. *Chem. Rev.* **2000**, *100*, 4567−4588.
(36) Gauthier, C.; Legault, J.; Pichette, A. *MROC* **2009**, *6*, 321−344.
(37) Sahu, N. P.; Achari, B. *Curr. Org. Chem.* **2001**, *5*, 315−334.
(38) Verli, H.; Guimarães, J. A. *Carbohydr. Res.* **2004**, *339*, 281−290.
(39) Becker, C. F.; Guimarães, J. A.; Verli, H. *Carbohydr. Res.* **2005**, *340*, 1499−1507.
(40) IUPAC-IUB Joint Commission on Biochemical Nomenclature. *Pure Appl. Chem.* **1996**, *68*, 1919−2008.
(41) Schuettelkopf, A. W.; van Aalten, D. M. F. *Acta Crystallogr. Sect. D* **2004**, *60*, 1355−1363.
(42) DeLano, W. L. *The PyMOL Molecular Graphics System*; DeLano Scientific LCC: San Carlos, CA, USA, 2002.
(43) Schaftenaar, G.; Noordik, J. H. *J. Comput.-Aided Mol. Des.* **2000**, *14*, 123−134.
(44) Van der Spoel, D.; Lindahl, E.; Hess, B.; Groenhof, G.; Mark, A. E.; Berendsen, H. J. C. *J. Comput. Chem.* **2005**, *26*, 1701−1718.
(45) Scott, W. R. P.; Hünenberger, P. H.; Tironi, I. G.; Mark, A. E.; Billeter, S. R.; Fennen, J.; Torda, A. E.; Huber, T.; Krüger, P.; van Gunsteren, W. F. *J. Phys. Chem. A* **1999**, *103*, 3596−3607.
(46) Pol-Fachin, L.; Fraga, C. A. M.; Barreiro, E. J.; Verli, H. *J. Mol. Graph. Model.* **2010**, *28*, 446−454.
(47) Berendsen, H. J. C.; Grigera, J. R.; Straatsma, T. P. *J. Phys. Chem.* **1987**, *91*, 6269−6271.
(48) Hess, B.; Bekker, H.; Berendsen, H. J. C.; Fraaije, J. G. E. M. *J. Comput. Chem.* **1997**, *18*, 1463−1472.
(49) Darden, T.; York, D.; Pedersen, L. *J. Chem. Phys.* **1993**, *98*, 10089−10092.
(50) Berendsen, H. J. C.; Postma, J. P. M.; DiNola, A.; Haak, J. R. *J. Chem. Phys.* **1984**, *81*, 3684−3690.
(51) Oostenbrink, C.; Villa, A.; Mark, A. E.; van Gunsteren, W. F. *J. Comput. Chem.* **2004**, *25*, 1656−1676.